

Prompt optical observations of Fermi-LAT bursts and GRB 090902B

S. B. Pandey, Carl W. Akerlof, W. Zheng and F. Yuan

Randall Laboratory of Physics, University of Michigan, Ann Arbor, Michigan, 48109-1040, USA

Observations of high energy emission from gamma-ray bursts (GRBs) constrain the extreme physical conditions associated with these energetic cosmic explosions. The Large Area Telescope (LAT) onboard the Fermi Gamma-ray Space Telescope, a pair conversion telescope, observes energetic quanta from 30 MeV to > 300 GeV. Synergy of the LAT with the Gamma-ray Burst Monitor (GBM) enlarges the energy coverage to ~ 7.5 decades, very useful for studying the GRB emission itself. Prompt optical observations and their possible correlations with photon emission at LAT energies help our understanding of the physical mechanisms behind these events. The prompt response times and large fields of of the ROTSE-III telescopes make afterglow observations possible for Fermi bursts with ~ 1 degree localized errors. As an example, GRB 090902B, was observed starting ~ 4803 s after the burst. This is the earliest ground-based optical detection ever made for long-duration bursts sensed by the LAT. The ROTSE detection classifies the optical afterglow of GRB 090902B as one of the brightest.

1. LAT GRBs and their importance:

The Fermi Gamma-ray Space Telescope has opened a new high-energy window in the study of GRBs. The understanding about the origin of high energy emission from GRBs is quite limited due to both the small number of bursts with known high energy photons and the small number of quanta that were detected in such cases, specially by the EGRET on board CGRO [1]. Observations of GRBs at the LAT energies will be able to not only constrain the nature of the prompt emission but will also help towards understanding the underlying radiation mechanism and the outflow composition [2]. There are a dozen GRBs which have been seen at LAT energies though more than ~ 300 GRBs have been detected by the GBM so far. For 6 of these bursts, the LAT boresight angle is < 65 degrees. Optical afterglows have been observed for 7 of these cases starting from ~ 16 hours after the burst and redshift values determined. So far, no prompt optical observations have been obtained for any one of the LAT-detected GRBs. In the past, near contemporaneous optical and gamma-ray observations of couple of GRBs have helped constrain the nature of prompt emission of these energetic cosmic explosions [3, 4].

2. GRB localization errors and their brightness:

The accuracy of localization of GRBs is not only a function of the detection technique used but also the brightness of the source at that energy. The onboard GBM has an angular resolution of 10 degrees whereas the LAT angular resolution is considerably better. The GRB localization errors computed by the method described in [5] are shown below in the left and right panels of Figure 1 for the expected number of photons and the GRB fluences with energies > 30 MeV respectively. For comparison, vertical lines show the bounds for some typical instruments that have

been used for rapid observations of GRB afterglows. A number of effects have been ignored such as the finite energy resolution of the calorimeter, degradation of the PSF for off-axis photons and the influence of PSF non-Gaussian tails. All of these will make the localization error larger. For this reason, the dotted lines show the effects of a reasonably optimistic degradation factor of 1.5.

Based on the simulated bursts, the localization accuracy was computed for both onboard and on-ground as a function of the expected number of counts at LAT frequencies [2] and are shown below respectively in the left and right panels of Figure 2. The results presented above in Figures 1 are similar to those presented in Figure 2. From Figure 2, it is clear that the number of identified GRBs and their localization accuracies are improved by the ground-based analysis but at the cost of considerable delay. These results further indicate the importance of ground-based robotic optical telescopes that can obtain early optical observations.

3. Optical Facilities and the LAT GRBs:

Extensive multi-wavelength observations of the LAT-detected GRBs (except bursts expected to be detected both by Swift/BAT and Fermi/LAT, for example GRB 090510) will only be possible if ground-based instruments identify these events efficiently. A dozen or so events per year with 100 LAT photons or more could be found by instruments with fields-of-view of 15 arcmin diameters for $\beta = -2.00$ and 24 arcmin diameters for $\beta = -2.25$. As shown in Figure 3 below, this requirement eliminates 61% (for $\beta = -2.00$) to 76% (for $\beta = -2.25$) of the observatories that have been reporting observations via GCN recently. Without the wider FoV systems such as RAPTOR, Super-LOTIS and ROTSE-III, the total discovery rate of such GRB afterglows may be restricted to 3-4 events per year. If Nature is uncooperative, this could be considerably less. With a FoV of $110' \times 110'$ and global coverage,

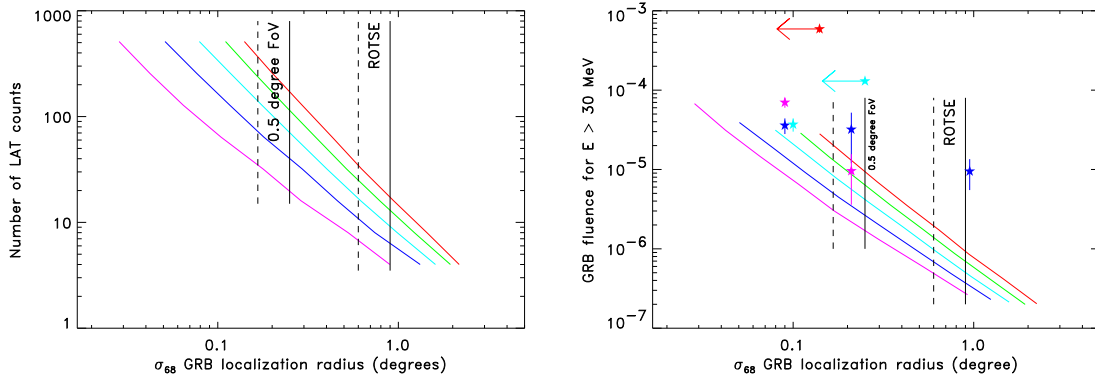


Figure 1: The number of required LAT-detected photons as a function of the median GRB localization error is shown in the left panel. The five lines indicate the behaviour for the spectral index $\beta = -2.00, -2.25, -2.50, -2.75$ and -3.00 , colour-coded from the top to bottom with an increasing values of β . The vertical lines show the cutoffs for instruments with 0.5 degree diameter FoV and ROTSE-III. In the right panel, the required GRB fluence for $E > 30$ MeV as a function of the median GRB localization error with five lines as described for the left panel of the Figure. Over plotted stars (colour coded to the nearest value of β determined for GRBs listed in Table 1) represent the 8 GRBs tabulated in Table 1. It is clear that most of such bursts would have been suitable for ground-based telescopes like ROTSE with the given LAT triggers.

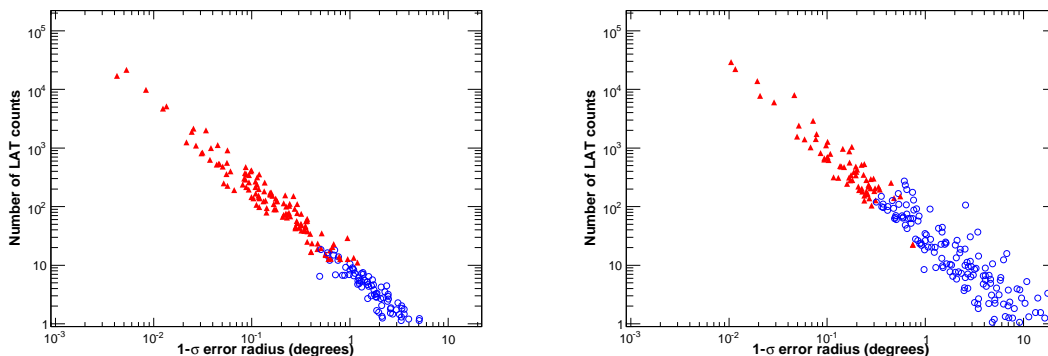


Figure 2: The localization accuracy of LAT onboard and on-ground along with expected number of the LAT photons are plotted in the left and right panels (The figures borrowed from [2]). In both the plots, the red triangles denote detected bursts and the open blue circles show undetected bursts.

ROTSE-III is much better matched to a broader range of spectral indices and fluences.

4. ROTSE Observations of the Fermi bursts:

The ROTSE-III telescopes have demonstrated their suitability for the near-simultaneous GRB observations at optical frequencies. Since launch of the Fermi, ROTSE-III has responded to many of the bursts commonly seen by Swift/BAT and Fermi/GBM and the near-simultaneous observations were made for 3 bursts, namely GRB 080810, GRB 080928 ([7], the poster presented in this meeting) and GRB 090618. There is no information about the LAT data for these 3 bursts. The LAT boresight angle is 61 degrees for

GRB 080810 and is 133 degrees for GRB 090618. GRB 090902B is the first LAT burst observed by ROTSE telescopes. The detail of observations and the properties of the burst are described below.

4.1. GRB 090902B:

The receipt of a ground-corrected GBM trigger [8] with a 1 degree nominal location error initiated an observing sequence for ROTSE-IIIa, located at the Siding Spring Observatory in Australia. The telescope began taking three sets of thirty 20-s images, around the GBM estimated location. Only the third set, starting ~ 80 minutes after the burst, with R.A. = 17h 38m 13s and Dec. = +27d 30' 59" covered the XRT burst location later identified as R.A. = 17h 39m 45.26s and Dec. = +27d 19' 28.1" [9]. A substantial

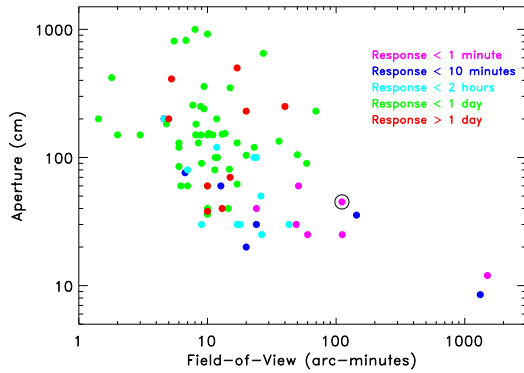


Figure 3: Scatter plot of 82 optical facilities producing GCN messages during 2005-2008. The colour code designates the minimum response time for the particular system. The parameters for the ROTSE-III instruments are identified by the circumscribed circle. The aperture (in cm) and field-of-view (in arcmin) were obtained from online documentation or relevant publications.

fraction of the delay was imposed by the interpolation of a previous observation request for an unrelated field. The images were processed using the standard ROTSE-III software pipeline and the unfiltered magnitudes were calibrated to R -band with respect to nearby USNO B1.0 stars using the method described in [10] and reported in [11].

Based on the statistical analysis of the total ensemble of 30 ROTSE-III measurements, we estimate a spurious detection probability of less than 1%. Combined with the spatial localization constraint, the probability of a false identification is less than 1×10^{-4} . The comparison of the optical brightness of GRB 090902B (extrapolating to 1000 sec after the burst) with the apparent optical brightness probability distribution function of well-observed afterglows [13] places this event among the top 3% of the brightest bursts observed so far. The burst is among the top 5% of bright bursts in the comparison of the brightness at 1000 sec with the compilation of light-curves of optical afterglows of pre-Swift and Swift-era GRBs with known redshifts [15].

4.2. Optical brightness of other LAT bursts:

Optical afterglows of other LAT-detected long-duration GRBs, except GRB 090902B, were obtained starting ~ 16 to 26 hours post-burst¹ and the redshift values were determined for most of them². Compar-

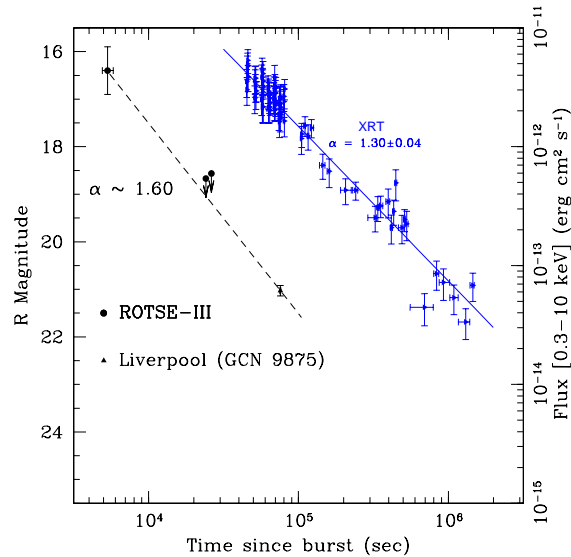


Figure 4: The afterglow lightcurve of GRB 090902B at optical and XRT frequencies. The optical observations seems decaying similar to LAT one [12] whereas XRT lightcurve decay rate is shallower. ROTSE observations are the earliest one ever taken for the long-duration GRBs by LAT.

ison of the optical brightness of these LAT-detected bursts with that of other well observed GRBs in the time-scales of 16 to 26 hours post-burst, indicate that they have a typical brightness as seen in the cases of pre-Swift and Swift GRBs [15]. The optical afterglow of GRB 090926 was exceptionally bright even at these later epochs [16].

5. Conclusions:

The estimation of the LAT localization errors as a function of the brightness of GRBs are presented. The analysis indicates the importance of ground-based robotic optical facilities for the multi-wavelength observations of these rare events. ROTSE-III observations of GRB 090902B indicate that the optical afterglow was one of the brightest at early epochs. Other LAT GRBs with measured redshifts, observed so far starting ~ 16 hours after the burst, share the typical optical brightness seen in case of Pre-Swift/Swift GRBs. More GRBs detected at the LAT energies and their follow-up observations will shed light on the early temporal properties of the afterglows and their possible correlation with the observed GeV emission.

Acknowledgments

This research has made use of the data obtained through the High Energy Astrophysics Sci-

¹<http://lyra.berkeley.edu/grbox/grbox.php>

²<http://www.mpe.mpg.de/jcg/grbgen.html>

Table I List of the 8 LAT-detected GRBs (Col. 1) with boresight angle < 65 degrees (Col. 2) and/or known redshifts (Col. 3). The Spectral index (Col. 4), the LAT fluence (Col. 5) [6] and the 1-sigma localization errors (Col. 6.) of these GRBs are over plotted in Figure 1. For more details, http://fermi.gsfc.nasa.gov/ssc/resources/observations/grbs/grb_table

Name of GRB	Boresight angle (in degrees)	Redshift (z)	Spectral index (β)	LAT fluence ($\text{egrs cm}^{-2} \text{sec}^{-1}$)	1-sigma LAT localization error radius (in degrees)
080825C	60	–	-2.34 ± 0.09	$(9.4 \pm 4) \times 10^{-6}$	0.95
080916C	48	4.35	-2.08 ± 0.06	$(7.0 \pm 1) \times 10^{-5}$	0.09
090323	–	3.57	–	$(3.6 \pm 0.8) \times 10^{-5}$	0.09
090328	–	0.74	-2.86 ± 0.10	$(3.2 \pm 2) \times 10^{-5}$	0.21
090510	–	0.90	-2.60 ± 0.30	$(3.7 \pm 0.7) \times 10^{-5}$	0.10
090626	15	–	-2.98 ± 0.02	$(9.6 \pm 6) \times 10^{-6}$	0.21
090902B	52	1.82	-3.85 ± 0.25	$(5.9 \pm 0.6) \times 10^{-4}$	< 0.14
091003	13	–	-2.64 ± 0.24	$(1.3 \pm 0.8) \times 10^{-5}$	< 0.25

ence Archive Research Center Online service, provided by the NASA/Goddard Space Flight Center. The ROTSE project is supported by the NASA grant NNX08AV63G and the NSF grant PHY-0801007.

References

- [1] Dingus B. L., 1995, *Ap&SS*, 231, 187
- [2] Band D., et al. 2009, *ApJ*, 701, 1673
- [3] Akerlof C. W. et al., 1999, *Nature*, 398, 400
- [4] Vestrand W. T. et al., 2006, *Nature*, 442, 172
- [5] Akerlof C. W. & Yuan F, 2006, [[arXiv:0702295](https://arxiv.org/abs/0702295)]
- [6] Ghisellini et al, 2009, Accepted to *MNRAS*, [[arXiv:09102459](https://arxiv.org/abs/09102459)]
- [7] Rossi E. et al., 2009, *The poster presented in this meeting*
- [8] Bissaldi E., & Connaughton V., 2009, *GCN Circ.*, 9866
- [9] Kennea, J., & Stratta, G., 2009, *GCN Circ.*, 9868
- [10] Quimby, R. M., et al., 2006, *ApJ*, 640, 402
- [11] Pandey, S. B., Zheng, W., et al., 2009, *GCN Circ.*, 9878
- [12] Abdo A. A. et al., 2009, *ApJ*, 706, L138
- [13] Akerlof C. W. & Swan H. F., 2007, *ApJ*, 671, 1868
- [14] Guidorazi C. et al., 2009, *GCN Circ.* 9875
- [15] Kann, A. et al., 2007, Submitted to *ApJ*, [[arxiv:0712218](https://arxiv.org/abs/0712218)]
- [16] Haislip J. et al., 2009, *GCN Circ.* 10003